Aberrant methylation of the *Pleckstrin and Sec7 domain-containing* gene is implicated in ulcerative colitis-associated carcinogenesis through its inhibitory effect on apoptosis

SHINICHIRO OKADA[1], KOICHI SUZUKI[1], KATO TAKAHARU[1], HIROSHI NODA[1], HIDENORI KAMIYAMA[1], TAKAFUMI MAEDA[1], MASAAKI SAITO[1], KEI KOIZUMI[2], YUICHIRO MIYAKI[2] and FUMIO KONISHI[1]

[1]Department of Surgery, Saitama Medical Center, Jichi Medical University, 1-847 Amanuma-cho, Omiya-ku, Saitama 330-8503; [2]First Department of Surgery, Hamamatsu University School of Medicine, 1-20-1 Handayama, Higashi-ku, Hamamatsu, Shizuoka 431-3192, Japan

Received August 2, 2011; Accepted September 28, 2011

DOI: 10.3892/ijo.2011.1231

Abstract. The *Pleckstrin and Sec7 domain-containing* (*PSD*) gene, which regulates skeletal rearrangements, has been found to be more frequently methylated both in ulcerative colitis (UC)-associated colorectal cancer tissues (5 of 7; 71.4%) and matched normal epithelia (4 of 7; 57.1%) compared to non-neoplastic UC epithelia (6 of 22; 27.3%) and sporadic colorectal cancer tissues (6 of 32; 18.8%). The levels of *PSD* mRNA were positively correlated with the methylation status of *PSD*, as shown by both MSP and bisulfite sequencing. To determine the potential role of *PSD* silencing in the mechanisms underlying UC-associated carcinogenesis, the levels of senescence, proliferation and apoptosis were evaluated in a normal human fibroblast cell line (NHDF) in which 93% of *PSD* expression was knocked down by a small-interfering RNA (si-RNA). Although there were no significant differences in the levels of senescence and proliferation caused by *PSD* knockdown, the level of apoptosis was significantly decreased by *PSD* knockdown (5.3% in siControl-treated cells vs. 0.67% in si*PSD*-treated cells, p=0.0001). In addition, reactive oxygen species inducers accelerated apoptosis in NHDF and a neutrophil-like cell line, which was significantly reduced by *PSD* knockdown. To verify the effect of *PSD* methylation in tissue sections including 21 samples from UC patients with or without tumors, we elucidated PSD promoting accumulation of filamentous-actin (F-actin) and apoptosis by immunohistochemistry and TUNEL assay, respectively. Both levels of accumulation of F-actin and apoptosis were significantly decreased in specimens from UC patients with *PSD* methylation compared to those without *PSD* methylation (F-actin: 0.69±0.86 with vs. 1.57±0.51 without, p=0.0031, apoptotic index: 0.31±0.63 with vs. 1.0±0.88 without, p=0.0277). In conclusion, our results indicate that *PSD* methylation plays a significant role in the mechanisms underlying UC-associated carcinogenesis through its inhibitory effect on apoptosis in the interaction between colorectal mucosa and neutrophils.

Correspondence to: Dr Koichi Suzuki, Department of Surgery, Saitama Medical Center, Jichi Medical University, 1-847 Amanuma-cho, Omiya-ku, Saitama 330-8503, Japan
E-mail: ksuzbnhm@yahoo.co.jp

Key words: promoter methylation, *Pleckstrin and Sec7 domain-containing* gene, ulcerative colitis-associated colorectal carcinogenesis, apoptosis, filamentous-actin, neutrophils

Introduction

Ulcerative colitis (UC) is a chronic inflammatory disease affecting the large intestine. Long-standing and extensive ulcerative colitis increases the risk of colorectal cancer (1,2). Due to improvements in the treatment of UC, mortality is now largely determined by the incidence of colorectal cancer, which emphasizes the need to detect early, pre-cancerous events occurring in patients with dysplastic epithelia or UC. The difficulty in surveillance colonoscopy (3) has encouraged the development of methods to identify early genetic and epigenetic alterations associated with UC-associated carcinogenesis (4). Discerning the mechanisms underlying UC-associated colorectal cancer will in turn improve the treatment and the prognosis of UC patients.

Epidemiological studies have indicated a link between chronic inflammation and carcinogenesis. For example, associations between chronic gastritis and hepatitis and stomach and liver cancers, respectively, have been shown (5-7). In these inflammatory diseases, aberrant methylation of promoter CpG islands is associated with the transcriptional inactivation of tumor suppressor genes (8). These epigenetic alterations have been observed not only in cancer tissues but also in tissues that appear to be histologically normal (9,10). Molecular alterations in non-neoplastic epithelia are more frequently observed in UC patients with neoplasia than in those without (11-13), supporting the view that they are involved in UC-associated carcinogenesis.

In this study, we used methylation-sensitive representational difference analysis (MS-RDA) to perform a comprehensive analysis of methylation alterations throughout the genome. This method was developed to enable a genome-wide search for differences in CpG methylation between cancer and

normal tissues (14). We show here that the *Pleckstrin and Sec7 domain-containing* (*PSD*) gene was frequently methylated in UC-associated carcinogenesis.

PSD is a guanine nucleotide exchange factor for ADP-ribosylation factor 6 (ARF6) (15), which regulates the membrane trafficking of small G proteins (16). PSD also regulates Ras-related C3 botulinum toxin substrate 1 (Rac 1), which is a Rho GTPase (15). Consequently, PSD coordinates endocytosis with cytoskeletal rearrangement by catalyzing nucleotide exchange on ARF6 and regulating Rac 1 activation (15). Although PSD inactivation has been reported to inhibit the transfer of G proteins into cells (15), no evidence of its association with carcinogenesis has been found. Based on the results herein, we suggest that *PSD* methylation plays a significant role in the mechanisms underlying UC-associated carcinogenesis.

Patients and methods

Patients and tissues. Seven UC-associated colorectal cancer tissues (UCT) with matched normal epithelia (UCN) and 22 non-neoplastic UC epithelia (UCI) were obtained from patients who had undergone surgery at Jichi Medical University Saitama Medical Center and Jichi Medical University Hospital from November 2000 to September 2006. The matched normal epithelia samples were taken from lesions harboring colitis adjacent to the tumors. In addition, 32 sporadic colorectal cancer tissues (SCC) without ulcerative colitis were obtained from patients who had undergone surgery. Eight normal colorectal epithelia (NC) were also obtained from patients who had undergone surgery for diverticulitis or appendicitis. This study was approved by the Ethics Committee of Jichi Medical University, and informed consent was obtained from each participant.

Cell line. The human skin fibroblast cell line (NHDF) was obtained from Kurabo (Osaka, Japan) and was maintained in Medium 106S supplemented with low serum growth supplement. The human promyelocytic leukemia cell line (HL-60), which look and behave like neutrophils, orient their polarity in response to a gradient and migrate in the right direction (17-19), were obtained from Japanese Collection of Research Bioresources (JCRB, Osaka, Japan). HL-60 cells were maintained in RPMI-1640 medium with 10% heat-inactivated fetal bovine serum.

Methylation-sensitive representational difference analysis. Tissue specimens were immediately soaked in RNAlater (Ambion, Austin, TX, USA) and stored at -80˚C until DNA or RNA extraction. MS-RDA was performed as previously described (14). Briefly, genomic DNA samples from cancerous and matched normal epithelia were digested by HpaII (New England Biolabs, Beverly, MA, USA), and the Rhpa adaptor was ligated to the resulting fragments. The HpaII-amplicon was then prepared by PCR. The Rhpa adaptor of the matched normal epithelium HpaII-amplicon was removed by MspI digestion, gel purified (Gel Extraction Kit; Qiagen, Hilden, Germany), and replaced by a JHpa adaptor. This amplicon was then mixed with an excess amount of the cancer tissue HpaII-amplicon to perform competitive hybridization, followed by PCR with the JHpa primers. After two cycles of competitive hybridization, the products were cloned into a pGEM-T Easy Vector (Promega, Madison, WI, USA). Sequence analysis of the plasmid DNA was performed using the T7 primer, Big Dye Terminator Cycle Sequencing Kit (Applied Biosystems, Carlsbad, CA, USA) and ABI PRISM 3100 Genetic Analyzer (Applied Biosystems).

Methylation-specific PCR and bisulfite sequencing analysis. Methylation-specific PCR (MSP) was performed as previously described (20) with slight modifications. The PSD primer sequences for the methylated reaction were 5'-CGTTAGGGGT TTTGAGTTTC-3' (forward) and 5'-ACCCCTAAACAAAC GTAACG-3' (reverse). The PSD primer sequences for the unmethylated reaction were 5'-TTTGTTAGGGGTTTTGAGT TTT-3' (forward) and 5'-TTACCCCTAAACAAACATAA CA-3' (reverse). PCR was performed for 35 cycles, consisting of denaturation at 94˚C for 30 sec, annealing at 55˚C for 30 sec, and extension at 72˚C for 60 sec, followed by a final 5-min extension at 72˚C for all primer sets. DNA samples were judged to be methylation positive if they yielded a visible PCR product after the MSP reaction. DNA sequencing was performed after bisulfite modification, as previously described (21). The primer sequences for the bisulfite sequencing were 5'-TTAGGA GGTTGTTATATGATTTG-3' (forward) and 5'-CTAAAATCTA ATTTAACATCCCC-3' (reverse). PCR was performed for 40 cycles, consisting of denaturation at 94˚C for 30 sec, annealing at 54˚C for 30 sec, and extension at 72˚C for 60 sec, followed by a final 5-min extension at 72˚C for all primer sets. The sequences were subjected to a BLAST search to determine their location in the genome.

Quantitative reverse transcription-PCR. Total RNA was immediately treated with DNase I (Invitrogen, Carlsbad, CA, USA) and reverse-transcribed using a Superscript II reverse transcriptase kit (Invitrogen) to prepare first-strand cDNA. The primer sequences for PSD were 5'-CCATAGACGAGGAGGAGCTG-3' (forward) and 5'-TCTTCCTGCAGTCAGGGTCT-3' (reverse). The thermal cycling conditions were 42˚C for 60 min (cDNA synthesis), 95˚C for 10 sec (hot start), and then 40 cycles of 95˚C for 5 sec, 58˚C for 10 sec, and 72˚C for 30 sec. The expression level of *PSD* was determined using the fluorescence intensity measurements from the ABI 7900HT Real-Time PCR System Data Analysis Software. A *GAPDH* fragment was amplified as an internal control.

Knockdown of PSD by small interfering RNA in HNDF and HL-60 cells. The *PSD*-specific siRNA (si*PSD*) was purchased from Invitrogen. RNA oligonucleotides were resuspended in 10 μM Tris-HCl, pH 8.0, 20 mM NaCl, and 1 mM EDTA to make a 20-μM siRNA solution. The final siRNA concentration was 30 nM in Opti-MEM I without serum. HNDF and HL-60 cells were cultured on or in dishes at 30-50% confluency without antibiotics and then transfection was performed with Lipofectamine 2000 (Invitrogen) according to the manufacturer's instructions. The BLOCK-iT™ Fluorescent Oligo (Invitrogen), which is a fluorescently labeled double-stranded RNA duplex with the same length, charge, and configuration, was used for the assessment of transfection efficiency and the Scrambled Stealth™ RNA molecule was used as the control siRNA (siControl). Cells were incubated for 48 h after transfection at 37˚C in a CO_2 incubator, then used for the subsequent experiments.

X-Gal cytochemical staining. To determine the level of senescence, X-Gal cytochemical staining for SA-β-Gal activity was performed with a Senescent Cells Histochemical Staining Kit (Sigma-Aldrich, St. Louis, MO, USA) according to the manufacturer's instructions. SA-β-Gal-positive cells were counted by eye and the average number of positive cells in random three fields was calculated.

Ki-67 immunohistochemistry. Immunohistochemistry for Ki-67 was performed using an anti-Ki-67 antibody (Lab Vision, Fremont, CA, USA) and the Histofine SAB-PO® Kit (Nichirei Bioscience, Tokyo, Japan) according to the manufacturer's instructions. Positive cells were counted by eye and the average number of positive cells in random three fields was calculated.

Detection of apoptotic cells in NHDF cells and in tissue sections. Apoptotic cells in NHDF cells were detected by terminal deoxynucleotidyl transferase (TDT)-mediated deoxyuridine triphosphate (dUTP) nick and labeling (TUNEL) using the ApopTag® Plus Fluorescein In Situ Apoptosis Detection Kit (Chemicon, Temecula, CA, USA) according to the manufacturer's instructions. The fluorescence signals were detected by a fluorescence microscope (Fluoview FV500; Olympus) with excitation at 490 nm and emission at 520 nm. The average number of positive cells in random three fields was calculated. To detect apoptotic cells in paraffin-embedded tissue sections, the sections were dewaxed in xylene and rehydrated with distilled water before using the ApopTag Plus Peroxidase In Situ Apoptosis Detection Kit, and tissue sections from 6 UCT, 6 UCN, and 15 UCI samples were used in this analysis. The apoptotic index was calculated using the percentage of labeled cells, with 0, +1, and +2 when less than 5%, 5-20%, and more than 20% of the cells demonstrated nuclear reactivity, respectively. While average of degrees taken from three regions of the colorectum (rectum, descending colon and ascending colon) was calculated as long as possible in UCN and UCI, one region around tumors was assessed as a representative of the degree in UCT.

Detection of active caspase-3/7. Active caspase-3/7 was detected by using the CaspaTag™ Caspase-3/7 Assay In Situ Assay Kit (Chemicon) according to the manufacturer's instructions. In order to accelerate apoptosis *in vitro*, after treatment with siControl or si*PSD* for 48 h, NHDF and HL-60 cells were exposed to reactive oxygen spices (ROS) inducers, pyocyanin (200 μM) for 30 min and lipopolysaccharide (LPS; 20 ng/ml) for 48 h, respectively. Then cells were subjected to the CaspaTag Caspase-3/7 assay and were stained with the CaspaTag reagent, a carboxyfluorescein-labeled fluoromethyl ketone peptide inhibitor of caspases-3 and -7 (SR-DEVD-FMK). The fluorescence signals were detected by a fluorescence microscope (Fluoview FV500; Olympus) with excitation at 550 nm and emission at 595 nm. The average number of caspase-3/7 positive cells in random three fields was calculated. LPS was purchased from Wako (Tokyo, Japan).

Detection of filamentous-actin. To detect filamentous-actin (F-actin) in paraffin-embedded tissue sections, immunocytochemical analysis of F-actin was performed using the I-VIEW DAB universal kit (Roche, Rotkreuz, Switzerland). The sections were dewaxed in xylene and rehydrated with distilled water before applying an immunohistochemical analysis of F-actin. The sections were treated with a heat-induced epitope retrieval technique using an EDTA buffer at pH 9.0 and blocked for endogenous peroxidase activity before applying the primary antibody. NH3 (Abcam, Tokyo, Japan) was used as a primary antibody for F-actin antibody. Incubation with a primary antibody was performed for overnight at 37˚C. Cells displaying slight staining of the cytoplasm were determined to be positive. A grading system was applied to the assessment of accumulation of F-actin in tissue sections. The F-actin index was calculated based on percentage of staining cell, with 0, +1, and +2 when less than -5% of cells, 5-20% cells, and more than 20% cells demonstrated cytoplasm reactivity, respectively. While average of degrees taken from three regions of the colorectum (rectum, descending colon and ascending colon) was calculated as long as possible in UCN and UCI, one region around tumors was assessed as a representative of the degree in UCT.

Statistical analysis. Statistical differences between variables were analyzed with unpaired t-tests or an analysis of variance, as appropriate. Simple regression coefficient analysis was used to examine associations between two categorical variables. The level of statistical significance was set at $p<0.05$.

Results

Clinicopathological features. The clinicopathological features of patients recruited for this study are shown in Tables I and II. The average age (40.1±15.3 years) of the UCI patients was significantly lower than that of the UCT (=UCN) (58.7±18.7 years), SCC (66.7±13.9 years), and NC patients (68.0±10.0 years, $p<0.05$). There was no significant difference in the average age between the following groups: UCT vs. SCC, SCC vs. NC, and NC vs. UCT. The disease duration of the UCI patients (8.0±5.0 years) was significantly shorter than that of the UCT patients (14.8±7.0 years, $p<0.05$).

Isolation of aberrantly methylated DNA fragments from UC-associated colorectal cancer tissues. To identify candidate genes involved in UC-associated carcinogenesis, MS-RDA was used to perform a genome-wide search for differences in CpG methylation between cancer and normal tissues. DNA obtained from a paired set of UCT and UCN samples was used as the tester and driver, respectively, for MS-RDA. A total of 23 DNA fragments were obtained, and the genomic location of each was confirmed by sequence analysis and a GenBank database search. Fifteen genes were located in CpG islands. Two genes, PSD and VAV3, were the guanine exchange factors for Rho GTPases. In particular, PSD was of interest because of its role in the coordination of membrane trafficking (15), which contributes to the adaptive immune system via its regulation (22). Disruption of this epithelial barrier function likely interferes with the host response to DNA damage caused by chronic inflammation.

PSD methylation and its down-regulation in UC-associated colorectal cancer tissues. The methylation analysis of *PSD* in 7 UCT and 2 control samples is shown in Fig. 1A. Aberrant methylation of *PSD* was detected in 5 of 7 UCT samples

Table I. Clinicopathological characteristics of non-neoplastic specimens from UC patients with and without colorectal cancer.

Group	*PSD*	Age	Gender	Duration	Onset	Ope
UCN1	M	77	M	13	64	Total
UCN2	M	40	M	8	32	Total
UCN3	M	64	F	9	55	Total
UCN4	U	35	M	15	20	Partial
UCN5	M	68	F	24	44	Total
UCN6	U	45	M	25	20	Total
UCN7	U	82	F	10	72	Right
UCI1	U	28	M	10	18	Total
UCI2	U	46	M	9	37	Total
UCI3	M	36	F	4	32	Total
UCI4	M	54	F	2	52	Total
UCI5	U	42	M	10	32	Total
UCI6	M	60	F	9	51	Total
UCI7	M	43	F	3	40	Total
UCI8	U	23	F	9	14	Total
UCI9	M	35	M	18	17	Total
UCI10	U	71	M	1.5	70	Total
UCI11	U	35	M	10	25	Total
UCI12	U	53	M	11	42	Total
UCI13	U	26	M	6	20	Total
UCI14	U	23	F	2	21	Total
UCI15	U	37	M	12	15	Total
UCI16	U	32	F	9	23	Total
UCI17	U	67	F	13	54	Total
UCI18	U	15	M	0.5	14	Total
UCI19	M	56	M	5	51	Total
UCI20	U	36	M	16	20	Total
UCI21	U	46	F	14	32	Total
UCI22	U	19	M	1.5	18	Total

UCT, UC-associated colorectal cancer tissues; UCN, matched normal epithelia; UCI, non-neoplastic UC epithelia; U in *PSD*, unmethylated; M in *PSD*, methylated; M in gender, male; F in gender, female; duration, disease duration (years); onset, age of onset (years); ope, operation; total, partial; and right in Ope, total colectomy, partial resection of the colon, and right hemi-colectomy, respectively.

(UCT1, -2, -3, -5, and -7). These findings were validated by bisulfite sequencing analysis (Fig. 1B, bottom). The degree of methylation alterations in 13 CpG sites located around the *PSD* transcription start site (Fig. 1B, top) was assessed in 7 UCT samples.

To verify the relationship between the methylation status of *PSD* and the levels of *PSD* mRNA, the relative expression levels of *PSD* in 7 UCT samples were quantified by real-time qRT-PCR and compared with those in NC. We observed a marked reduction in the levels of *PSD* mRNA in 5 of 7 UCT samples (Fig. 1C). The levels of *PSD* mRNA were positively correlated with the *PSD* methylation status (Fig. 1A and C).

Frequent methylation of PSD in UC-associated colorectal cancer tissues. The incidence of *PSD* aberrant methylation is shown in Fig. 2. Five of 7 UCT samples (71.4%), 4 of 7 UCN samples (57.1%), 6 of 22 UCI samples (27.3%), and 6 of 32 (18.8%) SCC samples were methylation positive, whereas no *PSD* aberrant methylation was detected in the 8 NC samples. Simple regression coefficient analysis revealed that no significant correlation was observed between age and *PSD* methylation.

Knockdown of PSD reduces apoptosis in NHDF cells. Approximately 86.0% of NHDF cells were transfected, and the level of toxicity caused by the transfection was 2.4%. The si*PSD* reduced the mRNA levels of *PSD* by 93%.

To investigate the biological significance of this epigenetic silencing of *PSD*, the levels of senescence, proliferation, and apoptosis were assessed in si*PSD*-treated NHDF cells. The value of histochemical SA-β-gal staining has been demonstrated by its ability to detect oncogene-induced senescence in murine and human premalignant neoplastic lesions (23). Thereby, to evaluate whether PSD methylation contributes to senescence, the level of senescence were determined by SA-β-gal staining. There was no significant difference in the level of senescence between siControl-treated NHDF cells and si*PSD*-treated NHDF cells (25.3% in siControl-treated cells vs. 23.2% in si*PSD*-treated cells, p=NS).

Because disruption of the balance between cell proliferation and cell death has been implicated in the initiation of several types of cancer (23), the levels of proliferation and apoptosis in NHDF cells after *PSD* knockdown were then assessed using Ki-67 immunostaining and TUNEL, respectively. There was no significant difference in the percentage of Ki-67-positive cells between siControl-treated NHDF cells and si*PSD*-treated NHDF cells (12.8% in siControl-treated cells vs. 15.3% in si*PSD*-treated cells, p=NS). In contrast, the percentage of apoptotic cells was significantly decreased in si*PSD*-treated cells when compared with siControl-treated cells (5.3% in siControl-treated cells vs. 0.67% in si*PSD*-treated cells, p=0.0001).

Knockdown of PSD inhibits the induction of apoptosis caused by reactive oxygen inducer in NHDF cells and HL-60 cells. Next, we elucidated whether *PSD* silencing inhibited pyocyanin or lipopolysaccharide (LPS)-induced apoptosis after transfection with siControl and si*PSD*. Since stimulation with LPS has no effect on fibroblast apoptosis *in vitro* (24), NHDF cells were treated with pyocyanin which released reactive oxygen species (ROS) mediated by redox reactions while HL-60 cells were treated with LPS which induced ROS via the activation of NADPH

Table II. Clinicopathological characteristics of tumor specimens from UC patients with colorectal cancer.

Group	*PSD*	Age	Gender	Duration	Onset	Loc	Type	Dukes	Ope
UCT1	M	77	M	13	64	R	Well	A	Total
UCT2	M	40	M	8	32	A	Muc	A	Total
UCT3	M	64	F	9	55	D	Well	A	Total
UCT4	U	35	M	15	20	D	Poor	D	Partial
UCT5	M	68	F	24	44	R	Well	B	Total
UCT6	U	45	M	25	20	D	Well	B	Total
UCT7	M	82	F	10	72	A	Poor	C	Right

UCT, UC-associated colorectal cancer tissues; UCN, matched normal epithelia; UCI, non-neoplastic UC epithelia; U in *PSD*, unmethylated; M in *PSD*, methylated; M in gender, male; F in gender, female; Duration, disease duration (years); Onset, age of onset (years); Loc, location of carcinoma; A, D and R in Loc, ascending colon, descending colon, and rectum, respectively; Type, histological findings of carcinoma; Well, poor, and muc in Loc, well-differentiated adenocarcinoma, poorly-differentiated adenocarcinoma, and mucinous adenocarcinoma, respectively; Dukes, Dukes' classification; Ope, operation; Total, partial, and right in Ope, total colectomy, partial resection of the colon, and right hemi-colectomy, respectively.

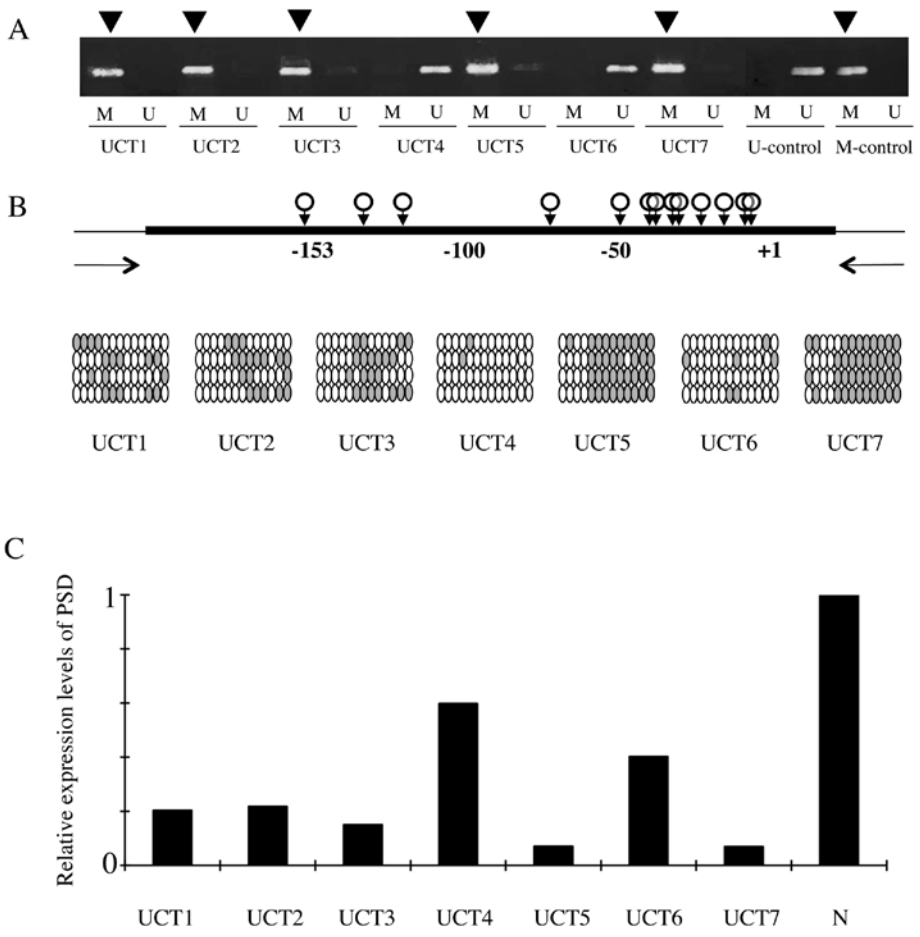

Figure 1. (A), Methylation analysis of *PSD* in 7 UCT and 2 control samples. The MSP products in lanes marked M show the presence of methylated templates (black arrow), whereas the products in lanes marked U show the presence of unmethylated templates. *PSD* aberrant methylation was detected in 5 of 7 (71.4%) UCT samples (UCT1, -2, -3, -5 and -7). UCT, UC-associated colorectal cancer tissues. U-control, unmethylated control DNA; M-control, methylated control DNA. (B), Schematic map of 13 CpGs around exon 1 of *PSD* (top) and bisulfite sequencing analysis of *PSD* (bottom). Open circles with arrows show CpG sites on the expanded axis. The transcription start site is marked with +1. The arrows represent the primers used in the MSP analysis, which were located from -231 to 10 nucleotides relative to the first exon based on the *PSD* cDNA sequence. The methylation status of each CpG site is indicated by closed (methylated) and open (unmethylated) circles. (C), Relative *PSD* expression levels in 7 UCT samples. The relative expression level of *PSD* was determined relative to the expression level of a normal colon epithelium.

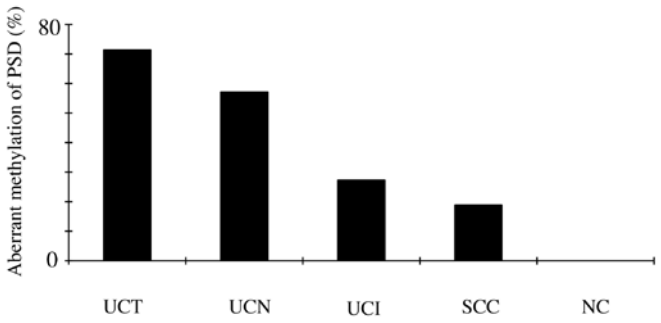

Figure 2. Incidence of *PSD* aberrant methylation detected by MSP in UCT, UCN, UCI, SCC, and NC samples. UCT, UC-associated colorectal cancer tissues; UCN, UC-associated colorectal cancer matched normal epithelia; UCI, non-neoplastic UC epithelia; SCC, sporadic colorectal cancer tissues; NC, normal colorectal epithelia.

oxidation. In this experiment, transfection efficiency was 89.1% in NHDF cells and 73.0% in HL-60 cells, which reduced the mRNA levels of *PSD* by 90.1% in si*PSD*-transfected NHDF and 61.3% in si*PSD*-transfected HL-60 cells, respectively. The average number of caspase-3/7 positive cells was significantly reduced in si*PSD*-treated NHDF cells when compared with siControl-treated NHDF cells (Fig. 3A; 30.33±3.29 in siControl vs. 2.67±1.02 in si*PSD*, p=0.0014). Likewise, the average number of caspase-3/7 positive cells was significantly reduced in si*PSD*-treated HL-60 cells when compared with siControl-treated HL-60 cells (Fig. 3B; 28.75±0.85 in siControl vs. 12.00±1.08 in si*PSD*, p<0.0001). Representative caspase-3/7-positive cells detected by the CaspaTag Caspase-3/7 assay in situ assay kit (Chemicon) and cell nucleus stained with Hoechst 33342 in NHDF cells and HL-60 cells treated with si*PSD* or siControl are shown in Fig. 3C and D.

The accumulation of filamentous-actin was decreased in tissue specimens from ulcerative colitis patients with PSD methylation. To determine the distribution of *PSD* inactivation by methylation in tissue specimens, PSD promoting accumulation of filamentous-actin (F-actin) was assessed by immunohistochemistry. The level of F-actin was significantly decreased in specimens from UC patients with *PSD* methylation when compared with those without (Fig. 4A; 0.69±0.86 with vs. 1.57±0.51 without, p=0.0031), suggesting that the accumulation of F-actin was inhibited by *PSD* methylation. This change was seen in not only colorectal mucosa but also inflammatory cells. Representative positive cells for F-actin in tissue specimens from UC patients without *PSD* methylation are shown in Fig. 4B.

The levels of apoptosis were significantly decreased in specimens from UC patients with PSD methylation. Next, we elucidated whether *PSD* methylation affected on the induction of apoptosis in tissue sections using 6 UCT, 6 UCN, and 15 UCI samples. The apoptotic index was significantly lower in UCN samples than in UCI samples (0 in UCN vs. 0.93±2.8 in UCI, p=0.011). The apoptotic index was significantly lower in UC patients with *PSD* methylation than in those without (Fig. 4C; 0.31±0.63 with vs. 1.0±0.88 without, p=0.0277). Representative apoptotic cells from the tissue sections are shown in Fig. 4D.

Discussion

The main findings of this study are that the aberrant methylation of *PSD* is frequently observed in UCT and UCN and that *PSD* silencing inhibits apoptosis *in vitro*. This inhibition of apoptosis was also observed in specimens from UC patients harboring *PSD* methylation. Taken together, these data indicate that the inhibition of apoptosis by *PSD* methylation likely plays a role in the mechanisms underlying UC-associated carcinogenesis.

Experimental and observational studies have provided genetic insights into the pathogenesis of inflammatory bowel disease (IBD). Affected genes are involved in the innate and adaptive immune system (25-27), autophagy pathway (28-30), epithelial barrier function (22,31), and endoplasmic reticulum stress response (32). A genome-wide association study identified genetic variants in Disks large homolog 5 (DLG 5) (22) that are associated with IBD. DLG 5 regulates cell shape, polarity (33) and cell-cell contact (34), and the disruption of these activities interferes with epithelial barrier function in the colon. The genome-wide analysis performed herein identified the *PSD* gene, which has similar roles such as coordinating cell shape and polarity.

Rac 1, a small Rho GTPase that is regulated by PSD (15), has been reported to play a pivotal role in the induction of apoptosis in the PSD-mediated signaling pathway. Fas-induced apoptosis is mediated by the activation of a Rac signaling pathway (35). UV-induced apoptosis was shown to be inhibited in Rat 2 fibroblasts harboring a dominant-negative RAC 1 mutant (36). In addition, Esteve *et al* demonstrated that Rho proteins, including Rho A, Rho C, and Rac 1, contribute to the physiological regulation of the apoptotic response to stress-inducing agents (37). These findings strongly support our data showing the inhibitory effect of *PSD* silencing on apoptosis *in vitro*. Some reports, however, have presented conflicting results (38-40), raising the possibility that Rac has a complex role, being involved in both the inhibition and stimulation of apoptosis.

Rho GTPases coordinate many cellular responses, often by regulating the formation of different actin assemblies (41). The inhibition of Rac has been shown to disrupt polarity or chemotaxis in polarized epithelial cells (42), fibroblasts (43), T cells (44), macrophages (45), and neutrophils (41). *PSD per se* also regulates actin and membrane remodeling (15). Our data, however, did not show which cells, epithelial or inflammatory cells, were responsible for the PSD-regulated apoptosis. Considering the short half-life of the neutrophils, it is unlikely that neutrophils would be methylated. Disturbance of the membrane ruffling of the colorectal mucosa by *PSD* methylation is likely implicated in disorder of immune system which interfers with the induction of chemoattractant to recruit and activate neutrophils. Both of these cells in specimens from UC patients harboring *PSD* methylation did not exhibit accumulation of F-action or apoptosis, suggesting that the inadequate interaction between these cells by disruption of PSD-regulated signaling pathways could play a crucial role in the mechanisms underlying UC-associated carcinogenesis, which might be exemplified by the 'field defect' caused by carcinogen exposure. To test this theory, further investigation is required.

Although all participants in this study were recruited in an unbiased manner during the same time period, the UCI patients

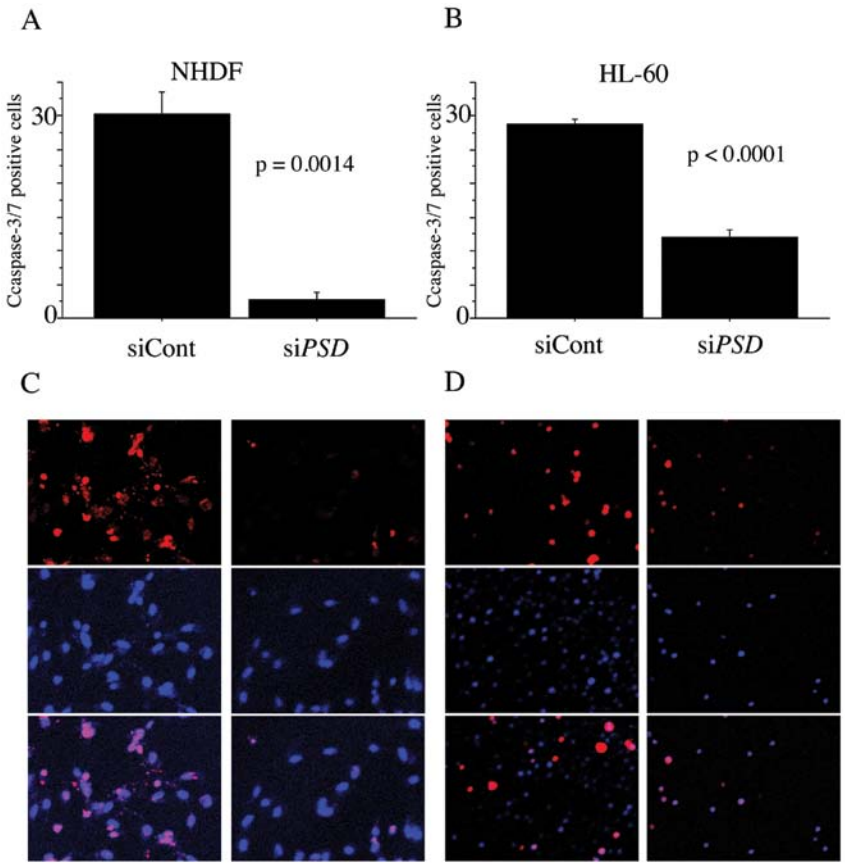

Figure 3. (A and B), Number of caspase-3/7 positive cells in siControl (siCont)-treated and si*PSD*-treated NHDF cells (A), and in siControl-treated and si*PSD*-treated HL-60 cells (B). In order to accelerate apoptosis, after treatment with siControl or si*PSD* for 48 h, NHDF and HL-60 cells were exposed to reactive oxygen spices (ROS) inducers, pyocyanin (200 μM) for 30 min and lipopolysaccharide (LPS, 20 ng/ml) for 48 h, respectively. (C), siControl-treated (left panel) and si*PSD*-treated NHDF cells (right panel) expressing active caspase-3/7 stained with CaspaTag Reagent (red, top) and their nuclear morphologic aspects stained with Hoechst 33342 (blue, middle), and those stained with both CaspaTag Reagent and Hoechst 33342 (pink, bottom). (D), siControl-treated (left panel) and si*PSD*-treated HL-60 cells (right panel) expressing active caspase-3/7 stained with CaspaTag Reagent (red, top) and their nuclear morphologic aspects stained with Hoechst 33342 (blue, middle), and those stained with both CaspaTag Reagent and Hoechst 33342 (pink, bottom).

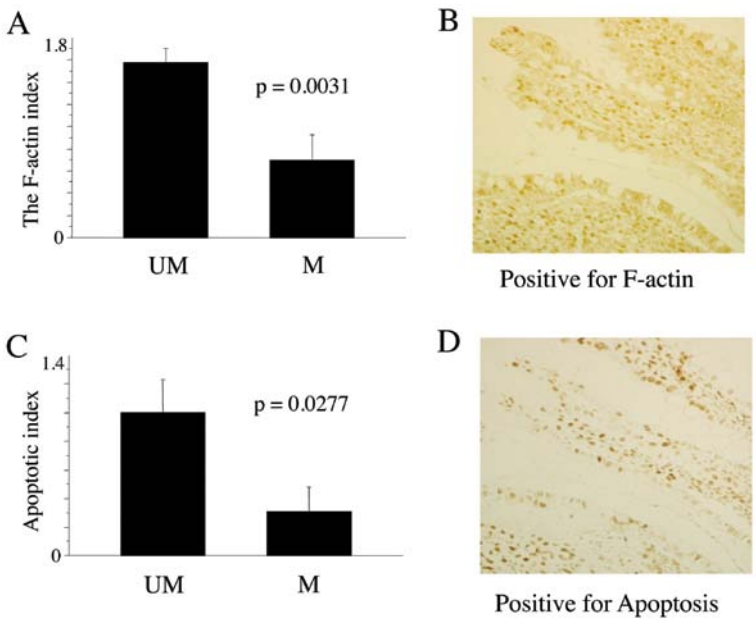

Figure 4. (A), The F-actin index in tissue specimens from UC patients with (M) and without *PSD* methylation (UM). For evaluation, three grades were determined as 0, +1, and +2 when less than -5% of cells, 5-20% cells, and more than 20% cells demonstrated cytoplasm reactivity, respectively. The average of degrees taken from three regions of the colorectum was calculated as long as possible. (B), Representative positive cells for F-actin in tissue specimens from UC patients without *PSD* methylation. (C), The apoptotic index in tissue specimens from UC patients with (M) and without *PSD* methylation (UM). The apoptotic index was calculated using the percentage of labeled cells, with 0, +1, and +2 when less than 5%, 5-20%, and more than 20% of the cells demonstrated nuclear reactivity, respectively. The average of degrees taken from three regions of the colorectum was calculated as long as possible. (D), Representative apoptotic cells detected by ApopTag in specimens from patients without *PSD* methylation.

were younger than the other patients. This observation raises the possibility that the *PSD* methylation frequently observed in UCT is caused by aging. Age-matched SCC patients and NC patients, however, exhibited a lower incidence of *PSD* methylation, suggesting that *PSD* methylation was unlikely to be age-dependent. Supporting the latter possibility, regression analysis showed no significant correlation between age and *PSD* methylation in this study. Because UCI patients generally suffer from refractory or persistent severe inflammation, they require operations at a younger age than do UCT patients. These earlier operations likely explain why UCI patients exhibit a shorter disease duration than do UCT patients. Patients harboring *PSD* methylation could escape from severe inflammation because of insufficient host response to inflammation, such as neutrophil-induced apoptosis, leading to long-term, persistent inflammation without an appropriate host response. Our findings are congruent with those reported by Kanmura *et al*, who showed that the levels of neutrophil peptide were significantly higher in patients with active UC than in patients whose UC was in remission and tended to be higher than those in patients with colon cancer (46).

UC-associated colorectal cancer progresses from areas of dysplastic mucosa (47,48) unlike sporadic colorectal cancer (49), which arises from adenomatous polyps. Dysplasia develops as a flat lesion, which makes it difficult to detect, especially in areas of active inflammation. Random biopsies are recommended in the British Society of Gastroenterology Guidelines (50), but estimates suggest that 33 and 66 biopsies are required to detect dysplasia with 90% and 95% confidence, respectively (51). Further investigation examining the association between dysplasia and *PSD* methylation may provide methods to estimate epigenetic damages occurring in inflammatory mucosa.

In conclusion, although the samples in this study are too limited to draw definitive conclusions, our results provide new and important information on the biological significance of *PSD* methylation in the mechanisms underlying UC-associated carcinogenesis through its inhibitory effect of apoptosis in interaction between colorectal mucosa and neutrophils.

Acknowledgments

This work was supported in part by a Grant-in-Aid for the post graduate student from Jichi Medical University and a Grant-in-Aid from the Ministry of Education, Culture, Sports, Science and Technology.

References

1. Ekbom A, Helmick C, Zack M and Adami HO: Ulcerative colitis and colorectal cancer. A population-based study. N Engl J Med 323: 1228-1233, 1990.
2. Lashner BA, Silverstein MD and Hanauer SB: Hazard rates for dysplasia and cancer in ulcerative colitis. Results from a surveillance program. Dig Dis Sci 34: 1536-1541, 1989.
3. Farraye FA, Odze RD, Eaden J, *et al*: AGA medical position statement on the diagnosis and management of colorectal neoplasia in inflammatory bowel disease. Gastroenterology 138: 738-745, 2010.
4. Garrity-Park MM, Loftus EV Jr, Sandborn WJ, Bryant SC and Smyrk TC: Methylation status of genes in non-neoplastic mucosa from patients with ulcerative colitis-associated colorectal cancer. Am J Gastroenterol 105: 1610-1619, 2010.
5. Eslick GD, Lim LL, Byles JE, Xia HH and Talley NJ: Association of *Helicobacter pylori* infection with gastric carcinoma: a meta-analysis. Am J Gastroenterol 94: 2373-2379, 1999.
6. Huang JQ, Sridhar S, Chen Y and Hunt RH: Meta-analysis of the relationship between *Helicobacter pylori* seropositivity and gastric cancer. Gastroenterology 114: 1169-1179, 1998.
7. Perz JF, Armstrong GL, Farrington LA, Hutin YJ and Bell BP: The contributions of hepatitis B virus and hepatitis C virus infections to cirrhosis and primary liver cancer worldwide. J Hepatol 45: 529-538, 2006.
8. Issa JP: CpG-island methylation in aging and cancer. Curr Top Microbiol Immunol 249: 101-118, 2000.
9. Kondo Y, Kanai Y, Sakamoto M, Mizokami M, Ueda R and Hirohashi S: Genetic instability and aberrant DNA methylation in chronic hepatitis and cirrhosis - a comprehensive study of loss of heterozygosity and microsatellite instability at 39 loci and DNA hypermethylation on 8 CpG islands in microdissected specimens from patients with hepatocellular carcinoma. Hepatology 32: 970-979, 2000.
10. Nakajima T, Maekita T, Oda I, *et al*: Higher methylation levels in gastric mucosae significantly correlate with higher risk of gastric cancers. Cancer Epidemiol Biomarkers Prev 15: 2317-2321, 2006.
11. Ahuja N, Li Q, Mohan AL, Baylin SB and Issa JP: Aging and DNA methylation in colorectal mucosa and cancer. Cancer Res 58: 5489-5494, 1998.
12. Brentnall TA, Crispin DA, Rabinovitch PS, *et al*: Mutations in the p53 gene: an early marker of neoplastic progression in ulcerative colitis. Gastroenterology 107: 369-378, 1994.
13. Ishitsuka T, Kashiwagi H and Konishi F: Microsatellite instability in inflamed and neoplastic epithelium in ulcerative colitis. J Clin Pathol 54: 526-532, 2001.
14. Ushijima T, Morimura K, Hosoya Y, *et al*: Establishment of methylation-sensitive-representational difference analysis and isolation of hypo- and hypermethylated genomic fragments in mouse liver tumors. Proc Natl Acad Sci USA 94: 2284-2289, 1997.
15. Franco M, Peters PJ, Boretto J, *et al*: EFA6, a sec7 domain-containing exchange factor for ARF6, coordinates membrane recycling and actin cytoskeleton organization. EMBO J 18: 1480-1491, 1999.
16. Macia E, Chabre M and Franco M: Specificities for the small G proteins ARF1 and ARF6 of the guanine nucleotide exchange factors ARNO and EFA6. J Biol Chem 276: 24925-24930, 2001.
17. Servant G, Weiner OD, Herzmark P, Balla T, Sedat JW and Bourne HR: Polarization of chemoattractant receptor signaling during neutrophil chemotaxis. Science 287: 1037-1040, 2000.
18. Servant G, Weiner OD, Neptune ER, Sedat JW and Bourne HR: Dynamics of a chemoattractant receptor in living neutrophils during chemotaxis. Mol Biol Cell 10: 1163-1178, 1999.
19. Wang F, Herzmark P, Weiner OD, Srinivasan S, Servant G and Bourne HR: Lipid products of PI(3)Ks maintain persistent cell polarity and directed motility in neutrophils. Nat Cell Biol 4: 513-518, 2002.
20. Herman JG, Graff JR, Myohanen S, Nelkin BD and Baylin SB: Methylation-specific PCR: a novel PCR assay for methylation status of CpG islands. Proc Natl Acad Sci USA 93: 9821-9826, 1996.
21. Frommer M, McDonald LE, Millar DS, *et al*: A genomic sequencing protocol that yields a positive display of 5-methylcytosine residues in individual DNA strands. Proc Natl Acad Sci USA 89: 1827-1831, 1992.
22. Stoll M, Corneliussen B, Costello CM, *et al*: Genetic variation in DLG5 is associated with inflammatory bowel disease. Nat Genet 36: 476-480, 2004.
23. Collado M and Serrano M: The power and the promise of oncogene-induced senescence markers. Nat Rev Cancer 6: 472-476, 2006.
24. Alikhani M, Alikhani Z, He H, Liu R, Popek BI and Graves DT: Lipopolysaccharides indirectly stimulate apoptosis and global induction of apoptotic genes in fibroblasts. J Biol Chem 278: 52901-52908, 2003.
25. Duerr RH, Taylor KD, Brant SR, *et al*: A genome-wide association study identifies IL23R as an inflammatory bowel disease gene. Science 314: 1461-1463, 2006.
26. Franke A, Balschun T, Karlsen TH, *et al*: Replication of signals from recent studies of Crohn's disease identifies previously unknown disease loci for ulcerative colitis. Nat Genet 40: 713-715, 2008.
27. Hugot JP, Chamaillard M, Zouali H, *et al*: Association of NOD2 leucine-rich repeat variants with susceptibility to Crohn's disease. Nature 411: 599-603, 2001.
28. Barrett JC, Hansoul S, Nicolae DL, *et al*: Genome-wide association defines more than 30 distinct susceptibility loci for Crohn's disease. Nat Genet 40: 955-962, 2008.

29. Hampe J, Franke A, Rosenstiel P, *et al*: A genome-wide association scan of nonsynonymous SNPs identifies a susceptibility variant for Crohn disease in ATG16L1. Nat Genet 39: 207-211, 2007.
30. Rioux JD, Xavier RJ, Taylor KD, *et al*: Genome-wide association study identifies new susceptibility loci for Crohn disease and implicates autophagy in disease pathogenesis. Nat Genet 39: 596-604, 2007.
31. Barrett JC, Lee JC, Lees CW, *et al*: Genome-wide association study of ulcerative colitis identifies three new susceptibility loci, including the HNF4A region. Nat Genet 41: 1330-1334, 2009.
32. Kaser A, Lee AH, Franke A, *et al*: XBP1 links ER stress to intestinal inflammation and confers genetic risk for human inflammatory bowel disease. Cell 134: 743-756, 2008.
33. Humbert P, Russell S and Richardson H: Dlg, Scribble and Lgl in cell polarity, cell proliferation and cancer. Bioessays 25: 542-553, 2003.
34. Wakabayashi M, Ito T, Mitsushima M, *et al*: Interaction of lp-dlg/KIAA0583, a membrane-associated guanylate kinase family protein, with vinexin and beta-catenin at sites of cell-cell contact. J Biol Chem 278: 21709-21714, 2003.
35. Gulbins E, Coggeshall KM, Brenner B, Schlottmann K, Linderkamp O and Lang F: Fas-induced apoptosis is mediated by activation of a Ras and Rac protein-regulated signaling pathway. J Biol Chem 271: 26389-26394, 1996.
36. Eom YW, Yoo MH, Woo CH, *et al*: Implication of the small GTPase Rac1 in the apoptosis induced by UV in Rat-2 fibroblasts. Biochem Biophys Res Commun 285: 825-829, 2001.
37. Esteve P, Embade N, Perona R, *et al*: Rho-regulated signals induce apoptosis *in vitro* and *in vivo* by a p53-independent, but Bcl2 dependent pathway. Oncogene 17: 1855-1869, 1998.
38. Boehm JE, Chaika OV and Lewis RE: Rac-dependent anti-apoptotic signaling by the insulin receptor cytoplasmic domain. J Biol Chem 274: 28632-28636, 1999.
39. Joneson T and Bar-Sagi D: Suppression of Ras-induced apoptosis by the Rac GTPase. Mol Cell Biol 19: 5892-5901, 1999.
40. Nishida K, Kaziro Y and Satoh T: Anti-apoptotic function of Rac in hematopoietic cells. Oncogene 18: 407-415, 1999.
41. Srinivasan S, Wang F, Glavas S, *et al*: Rac and Cdc42 play distinct roles in regulating PI(3,4,5)P3 and polarity during neutrophil chemotaxis. J Cell Biol 160: 375-385, 2003.
42. Kroschewski R, Hall A and Mellman I: Cdc42 controls secretory and endocytic transport to the basolateral plasma membrane of MDCK cells. Nat Cell Biol 1: 8-13, 1999.
43. Nobes CD and Hall A: Rho GTPases control polarity, protrusion, and adhesion during cell movement. J Cell Biol 144: 1235-1244, 1999.
44. Haddad E, Zugaza JL, Louache F, *et al*: The interaction between Cdc42 and WASP is required for SDF-1-induced T-lymphocyte chemotaxis. Blood 97: 33-38, 2001.
45. Allen WE, Zicha D, Ridley AJ and Jones GE: A role for Cdc42 in macrophage chemotaxis. J Cell Biol 141: 1147-1157, 1998.
46. Kanmura S, Uto H, Numata M, *et al*: Human neutrophil peptides 1-3 are useful biomarkers in patients with active ulcerative colitis. Inflamm Bowel Dis 15: 909-917, 2009.
47. Nugent FW, Haggitt RC and Gilpin PA: Cancer surveillance in ulcerative colitis. Gastroenterology 100: 1241-1248, 1991.
48. Woolrich AJ, Da Silva MD and Korelitz BI: Surveillance in the routine management of ulcerative colitis: the predictive value of low-grade dysplasia. Gastroenterology 103: 431-438, 1992.
49. Burmer GC, Rabinovitch PS, Haggitt RC, *et al*: Neoplastic progression in ulcerative colitis: histology, DNA content, and loss of a p53 allele. Gastroenterology 103: 1602-1610, 1992.
50. Farraye FA, Odze RD, Eaden J and Itzkowitz SH: AGA technical review on the diagnosis and management of colorectal neoplasia in inflammatory bowel disease. Gastroenterology 138: 746-774, 2010.
51. Rubin CE, Haggitt RC, Burmer GC, *et al*: DNA aneuploidy in colonic biopsies predicts future development of dysplasia in ulcerative colitis. Gastroenterology 103: 1611-1620, 1992.